ARTICLE

Obesity-induced hyperglycemia impairs oral tolerance induction and aggravates food allergy

Lícia Torres [1], Mariana Camila Gonçalves Miranda [1,2], Vinícius Dantas Martins [1], Felipe Caixeta [1], Mariana de Almeida Oliveira [1], Luísa Martins Trindade [3], Helder Carvalho de Assis [1,4], Valbert Nascimento [3], Natália Pinheiro Rosa [1], Eliane Gomes [5], Sophia Oliveira Almeida [1], Florian Marquet [6], Laurent Genser [8,9], Genevieve Marcelin [6], Karine Clément [8,9], Momtchilo Russo [5], Ana Maria Caetano Faria [1] and Tatiani Uceli Maioli [1,7,✉]

Obesity and type 2 diabetes (T2D) have been found to be associated with abnormalities in several organs, including the intestine. These conditions can lead to changes in gut homeostasis, compromising tolerance to luminal antigens and increasing susceptibility to food allergies. The underlying mechanisms for this phenomenon are not yet fully understood. In this study, we investigated changes in the intestinal mucosa of diet-induced obese mice and found that they exhibited increased gut permeability and reduced Treg cells frequency. Upon oral treatment with ovalbumin (OVA), obese mice failed to develop oral tolerance. However, hyperglycemia treatment improved intestinal permeability and oral tolerance induction in mice. Furthermore, we observed that obese mice exhibited a more severe food allergy to OVA, and this allergy was alleviated after treatment with a hypoglycemic drug. Importantly, our findings were translated to obese humans. Individuals with T2D had higher serum IgE levels and downregulated genes related to gut homeostasis. Taken together, our results suggest that obesity-induced hyperglycemia can lead to a failure in oral tolerance and to exacerbation of food allergy. These findings shed light on the mechanisms underlying the relationship among obesity, T2D, and gut mucosal immunity, which could inform the development of new therapeutic approaches.

Mucosal Immunology (2023) 16:513–526; https://doi.org/10.1016/j.mucimm.2023.05.008

INTRODUCTION

Obesity is a complex disease associated with numerous metabolic and inflammatory disorders, including cardiovascular disease, dyslipidemia, type 2 diabetes (T2D), autoimmune diseases, cancer, and altered immune responses[1,2]. The immunological changes related to obesity are primarily caused by alterations in the adipose tissue structure and the increased secretion of inflammatory compounds by adipocytes. These changes result in heightened secretion of proinflammatory cytokines, such as tumor necrosis factor (TNF)-α, interleukin-1β (IL-1β), IL-6, IL-8, leptin, and resistin, and a parallel reduction in anti-inflammatory cytokines, such as IL-10 and adiponectin. As a result, obesity is characterized as a low-intensity inflammatory state that can impact immune compartments such as the intestinal mucosa[3,4].

The effects on the gut mucosa immune system due to obesity have been associated with increased levels of interferon (IFN)γ-producing cells and alterations in gut permeability in humans and mice[5]. In humans, obesity enhances jejunal inflammation, resulting in an increased frequency of macrophages, T cells (clusters of differentiation [$CD3^+$]), intraepithelial lymphocytes, and mature dendritic cells (mDCs). These cells produce proinflammatory cytokines such as IFN-γ, IL-1β, TNF-, chemokines, and costimulatory factors, which contribute to inflammation in the gut lamina propria and epithelial compartments[6].

The intestinal mucosa is the largest contact surface of the body with the external environment[7], and its immune cells face the challenge of tolerating the vast number of antigens that come from diet and commensal microbiota while generating protective immune responses against intestinal pathogens and toxins[8].

The immune system's ability to maintain homeostasis is a delicate balance between proinflammatory and anti-inflammatory responses. This balance is particularly crucial in the gut mucosal surface, where the development of regulatory responses is essential for the induction of oral tolerance to dietary proteins

[1]Departamento de Bioquímica e Imunologia, Instituto de Ciencias Biológicas, Universidade Federal de Minas Gerais, Belo Horizonte, Brazil. [2]Elliot and Roslyn Jaffe Food Allergy Institute Icahn School of Medicine at Mount Sinai, New York, USA. [3]Programa de Pós-Graduação em Ciências dos Alimentos, Faculdade de Farmácia, Universidade Federal de Minas Gerais, Belo Horizonte, Brazil. [4]Laboratório de Imuno-inflamação, Departamento de Genética, Evolução, Microbiologia e Imunologia, Instituto de Biologia, Universidade de Campinas, Campinas, Brazil. [5]Laboratório de Imunobiologia, Departamento de Imunologia, Instituto de Ciências Biomédicas, Universidade de São Paulo (ICB/USP), São Paulo, Brazil. [6]Sorbonne Université, INSERM, Nutrition et Obesities; Systemic Approaches, NutriOmique, Paris, France. [7]Departamento de Nutrição, Escola de Enfermagem, Universidade Federal de Minas Gerais, Belo Horizonte, Brazil. [8]Sorbonne Université, INSERM, Nutrition et Obesities; systemic approaches, NutriOmique, Assistance Publique-Hôpitaux de Paris, Nutrition Department, Hôpital Pitié-Salpêtrière, Paris, France. [9]Sorbonne Université, INSERM, Nutrition et Obesities; systemic approaches, NutriOmique, Assistance Publique-Hôpitaux de Paris, Visceral Surgery Department, Hôpital Pitié-Salpêtrière, Paris, France. ✉email: tatianimaioli@gmail.com

Received: 21 December 2022 Accepted 16 May 2023
Published online: 10 June 2023

and the microbiota. Oral tolerance is a physiologic phenomenon that is defined as an anti-inflammatory immune response to specific antigens that are orally administered. This response has both local and systemic effects, and it plays a critical role in maintaining gut mucosal immune homeostasis[9].

Oral tolerance is a physiological phenomenon that prevents pathological inflammatory reactions to a food protein and commensal microbiota, inhibiting responses that could cause damage, such as hypersensitivity reactions, lymphocyte proliferation, and antibody formation[9]. Orally administered antigens promote subsequent tolerogenic immune responses that act locally and systemically and can attenuate inflammatory and harmful cellular and humoral immune responses[10,11]. The main mechanisms involved in developing oral tolerance are the generation of tolerogenic dendritic cells (DCs)[12,13] and the differentiation of Foxp3-expressing regulatory T cells[14,15] that inhibit specific cellular[16,17] and humoral[10] responses. Induced $Foxp3^{+}CD4^{+}$ regulatory T cells act via the production of inhibitory cytokines, such as IL-10 and transforming growth factor (TGF)-β[16]. However, several factors, including obesity, can disrupt this delicate balance, leading to the breakdown of oral tolerance and the activation of proinflammatory responses, such as food allergy.

Food allergy affects approximately 10% of the population[18], and this number could be increased by the high obesity prevalence[19], it occurs as a consequence of the disruption in immunological tolerance to ingested food resulting from either immunoglobulin (Ig)E-mediated or non–IgE-mediated disorders[20]. Immediate hypersensitivity reactions occur through the cross-linking between the IgE-FcεRI complex by the allergen, resulting in mast cell degranulation and the release of lipid mediators such as prostaglandins and leukotrienes, cytokines, and chemokines, characterizing the initial phase of the allergic reaction. Cytokines and chemokines released in the initial phase start the late phase, represented by the recruitment and activation of inflammatory cells, mainly eosinophils, and Th2 lymphocytes, at the sites of antigen sensitization[21].

Previous studies from our group have demonstrated that mice fed a high-sugar and high-fat diet (HSB) exhibit a reduction in the frequency of regulatory T cells and a decrease in the secretion of anti-inflammatory cytokines such as IL-10 and TGF-β[22]. Diets that are low in fiber and high in sugar and fat have been implicated in the pathogenesis of obesity, as they can increase gut permeability, inflammation, and dysbiosis, ultimately leading to the disruption of gut homeostasis[4,23]. Obesity and food allergies have been associated in epidemiological evidence[19,24], and the involvement between those conditions can be associated with a high-fat diet and gut microbial alterations[19,25]. However, how obesity changes gut immune homeostasis and compromises oral tolerance induction has not been clearly reported. Thus, the impact of obesity and its metabolic alterations, such as hyperglycemia, could implicate failure in oral tolerance induction or breakdown of existing tolerance mechanisms; in addition, it can result in immunopathology[26], such as food allergy.

To test this hypothesis, we evaluated the effect of obesity and hyperglycemia on oral tolerance induction and food allergy development. We showed that obesity-induced hyperglycemia in mice was associated with alterations in the gut immune system, impairment of oral tolerance induction, and aggravation of food allergy. Furthermore, we showed that obesity associated with type T2D in humans correlated with higher IgE serum levels and increased markers of gut homeostasis disruption. Understanding the mechanisms involved in obesity and oral tolerance imbalance will enable the development of novel approaches for oral tolerance-based therapies and treatment for food allergy.

RESULTS

Diet-induced obesity disturbed gut homeostasis in mice

Experimental obesity was induced in C57BL/6 mice by feeding them an HSB diet, while lean control mice (CTL) were fed the AIN93G[26] diet for 13 weeks. The HSB-fed mice exhibited a significant increase in body weight after just 5 weeks of consumption compared to the AIN93G-fed lean mice (Fig. 1A), and this difference continued to widen throughout the study. The obese mice also demonstrated a higher epididymal adipose tissue index and adipose tissue hypertrophy (Supplementary Figs. 1A–D). Hyperglycemia was observed in the obese mice as early as 5 weeks after consuming the HSB diet (Fig. 1B). After 13 weeks, the obese mice developed glucose intolerance compared to the control lean mice (Supplementary Figs. 1E–F), and their fasting blood glucose levels were consistent with those observed in type 2 diabetes (Fig. 1B). Furthermore, the obese mice exhibited features of metabolic syndrome, such as elevated levels of circulating triglycerides and total cholesterol, as well as hepatic steatosis (Supplementary Figs. 1G–I).

Fig. 1 HSB diet-induced obesity is associated with metabolic and gut mucosa alterations. Mice were treated for 13 weeks with a control diet (AIN93G) or a diet containing high concentrations of butter and sugar (HSB), then mice were euthanized and all following analysis procedures. (A) Mice body weight over 13 weeks of treatment comparing non-obese mice (CTL - represented as black circles) to obese mice (HSB - represented as red squares). (B) Fasting blood glucose concentrations in CTL (represented as circles) and HSB-fed mice (obese mice represented as squares) from 5 weeks and 13 weeks of diet treatment (N = 6 to 8). (C) Plasma concentration of ^{99}mTc-DTPA to indicate intestinal permeability (N = 5 to 11). (D) sIgA concentrations in feces measured by enzyme-linked immunosorbent assay (N = 5). (E) IgA coated-bacteria recovered from feces (N = 8). (F) IgA coated-bacteria representative plots from flow cytometer. (G) Phenotypic characterization of TCRαβ IELs in the small intestine (each point represents two mice). (H) Representative plots from TCRαβ IELs. (I) Frequencies of $CD4^{+}$ T cells from *lamina propria* (each point represents two mice). (J) Representative plots of frequencies of $CD4^{+}$ T cells in the *lamina propria.* (K) Frequency of $CD4^{+}Foxp3^{+}$ cells from compartmentalized mLN. Each point represents three mice. (L) Representative plots of $CD4^{+}Foxp3^{+}$ cells frequencies from mLN (duodenal, jejunal, ileum, and colon). (M) Frequency of $CD103^{+}CD11b^{-}$ DC from compartmentalized mLN (each point represents two mice). (N) *Tsne* plots of DC from the duodenum and ileum lymph nodes. Data represent the mean ± standard deviation. (*) $p < 0.05$; (**) $p < 0.01$; (***) $p < 0.001$. Data represent two independent experiments. White bars represent control mice (CTL), and grey bars represent obese mice (HSB). ^{99}mTc-DTPA = 99 m-technetium diethylenetriamine penta-acetic acid; CD = clusters of differentiation; CTL = lean control mice; DC = dendritic cells; HSB = high-sugar and high-fat die; IEL = intraepithelial lymphocyte; Ig = immunoglobulin; mLN = mesenteric lymph nodes; sIgA = secretory IgA; TCR = T Cell Receptor.

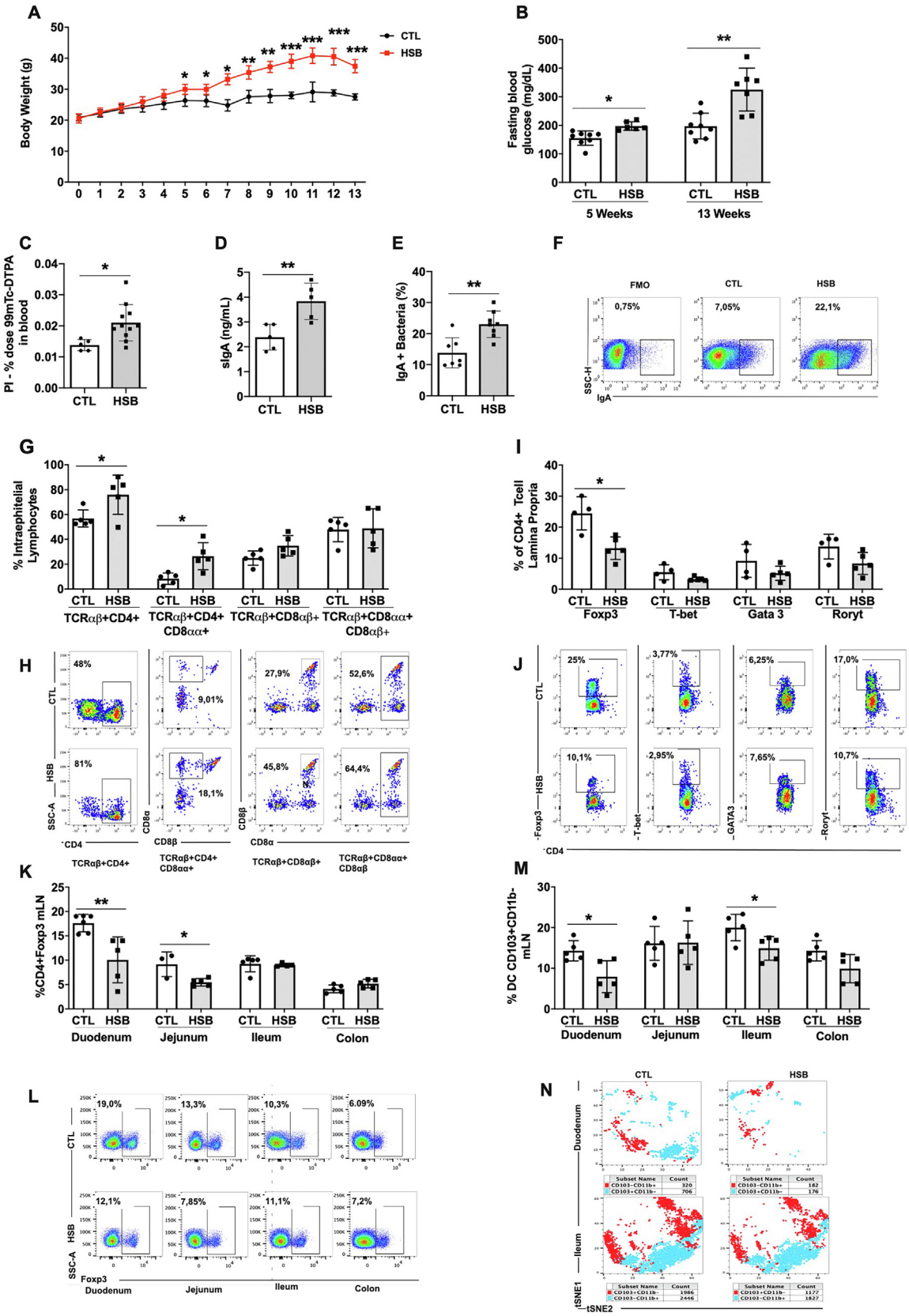
A
Body Weight (g)
CTL
HSB
B
Fasting blood glucose (mg/dL)
5 Weeks
13 Weeks
C
PI - % dose 99mTc-DTPA in blood
D
sIgA (ng/mL)
E
IgA + Bacteria (%)
F
FMO
CTL
HSB
0,75%
7,05%
22,1%
SSC-H
IgA
G
% Intraephitelial Lymphocytes
TCRαβ+CD4+
TCRαβ+CD4+ CD8αα+
TCRαβ+CD8αβ+
TCRαβ+CD8αα+ CD8αβ+
I
% of CD4+ Tcell Lamina Propria
Foxp3
T-bet
Gata 3
Roryt
H
48%
9,01%
81%
18,1%
27,9%
45,8%
52,6%
64,4%
SSC-A
CD4
CD8α
CD8β
J
25%
3,77%
6,25%
17,0%
10,1%
2,95%
7,65%
10,7%
Foxp3
T-bet
GATA3
Roryt
K
%CD4+Foxp3 mLN
Duodenum
Jejunum
Ileum
Colon
M
% DC CD103+CD11b- mLN
L
19,0%
13,3%
10,3%
6.09%
12,1%
7,85%
11,1%
7,2%
Foxp3
N
Duodenum
Ileum
tSNE1
tSNE2
Subset Name
Count
CD103+CD11b+
CD103+CD11b-
320
706
182
176
1986
2446
1177
1827

Our study examined the impact of an HSB on gut permeability in mice. We found that HSB-fed mice had significantly higher gut permeability than the control group (Fig. 1C). Further analyses revealed that obese mice exhibited increased levels of secretory IgA (sIgA) and higher frequencies of IgA-coated bacteria, suggesting an altered gut immune response (Fig. 1D–F). We also observed an increase in the number of goblet cells, which are important for mucus production and barrier function (Supplementary Fig. 1K). Moreover, flow cytometry analysis revealed alterations in the frequencies of TCRβ$^+$CD4$^+$ and TCRβ$^+$CD4$^+$-CD8αα$^+$ intraepithelial lymphocytes in obese mice (Fig. 1G and 1H), and these results were consistent with the histopathological findings (Supplementary Fig. 1L).

We also examined the frequencies of regulatory T cells CD4$^+$-Foxp3$^+$ (Tregs) and dendritic cells (DCs) in the lamina propria and mesenteric lymph nodes (mLNs), including the draining lymph nodes of the duodenum, jejunum, ileum, and colon. Our analysis revealed a significant reduction in the frequency of Treg cells in the lamina propria, duodenal, and jejunal lymph nodes of obese mice, whereas no significant difference was observed in the ileum and colon draining lymph nodes (Fig. 1I–L). In addition, the frequencies of CD103$^+$CD11b$^-$ conventional dendritic cells (cDCs), which are known to be effective in differentiating induced Treg cells (iTregs), were lower in the duodenum and ileum draining lymph nodes of obese mice (Fig. 1M and N). No significant difference was found in the frequencies of DCs and innate lymphoid cells (ILCs) in the lamina propria (Supplementary Fig. 1M-Q). Furthermore, obese mice exhibited a decreased frequency of CD19$^+$ cells in the spleen, but no significant difference was observed in the mLNs (Supplementary Fig. 1R). These findings suggest that the gut of obese mice is characterized by an inflammatory environment and a loss of intestinal homeostasis.

Obesity impaired oral tolerance induction in mice

Given the importance of gut mucosa homeostasis to oral tolerance development, we speculated whether the alterations in the intestinal mucosa of obese mice could impact oral tolerance induction. To test this hypothesis, we treated control lean and obese mice orally with a single gavage of 10 mg of ovalbumin (OVA), followed by immunization containing OVA-Alum (10 μg of OVA plus 1 mg of alum via intraperitoneal [i.p.]), and a subsequent booster. As a protocol control, mice received a gavage containing saline and then received the same immunization scheme; this group was called the saline group (Fig. 2A).

Indeed, the control group had reduced titers of total specific antibodies as well as IgG1 and total IgE after OVA treatment; on the other hand, obese mice were resistant to oral tolerance induction, as shown by their higher levels of specific serum IgG1 and total IgE after oral OVA treatment (Fig. 2B and 2C). IgG2a and IgM did not change after oral OVA treatment in either group (Supplementary Figs. 2A and 2B). The specific cellular immune response was also analyzed. Cells from the spleen and mLNs were isolated and stimulated *in vitro* with OVA, and the cytokines were measured in the supernatants. The levels of IFN- γ were higher in the spleen and mLN cell supernatants from OVA-fed obese mice than in those from control lean mice (Fig. 2D; Supplementary Fig. 2C). We also observed increased levels of TNF-α in the spleen cell supernatants from obese mice that received OVA (Fig. 2E). However, TFG-β levels were increased only in OVA-fed control lean mice (Fig. 2F). In addition, we evaluated the frequency of CD4$^+$Foxp3$^+$, CD4$^+$Ror γt$^+$, CD4$^+$T-bet$^+$, and CD4$^+$GATA3$^+$ T cells in mLNs, an important site for oral tolerance development, and in the spleen, which represents the systemic response of the oral tolerance induction phenomenon. Regarding the frequency of the cells, OVA-fed lean control mice, but not OVA-fed obese mice, had an increased frequency of CD4$^+$Foxp3$^+$ regulatory T cells in duodenal lymph nodes and spleen (Fig. 2G; Supplementary Fig. 2E). T helper (Th)17 (CD4$^+$-ROR γT$^+$) cells decreased in the dLN from OVA-fed lean control mice, and OVA-fed obese mice showed an increased frequency of those cells (Fig. 2H). No differences were observed for CD4$^+$-ROR γT$^+$cells in the spleen (Supplementary Fig. 2G). CD4$^+$T-bet$^+$ T-cell frequency decreased in OVA-fed lean mice in the spleen but not in the dLN. No difference was observed in the OVA-fed obese mice (Supplementary Figs. 2H and 2K). After oral tolerance induction, lean mice also presented an increased frequency of tolerogenic CD103$^+$CD11b$^-$DCs, while obese mice did not show a difference in this cell population in the spleen (Fig. 2I). Thus, these data showed alterations in the humoral and cellular responses of obese mice after oral treatment with OVA, suggesting that obesity has a deleterious effect on oral tolerance induction.

Treatment of hyperglycemia restored oral tolerance induction in obese mice

Our research group previously demonstrated that nonobese diabetic (NOD) mice, which serve as a model for type 1 diabetes (T1D), exhibit a refractory response to oral tolerance induction[27]. Building on this finding, we investigated whether obese mice with type 2 diabetes (T2D) also display a similar refractory response to oral tolerance induction. To examine the effect of hyperglycemia on gut permeability and the ability to induce oral tolerance, we utilized a nonobese hyperglycemic animal model induced by streptozotocin (STZ) treatment administered i.p. at a dose of 50 mg/kg for 5 consecutive days. Seven days after the last STZ injection, fasting glucose reached more than 250 mg/dl, indicating hyperglycemia (Supplementary Figs. 3A–C). STZ-treated mice presented higher intestinal permeability than control mice, and gut permeability was positively correlated with glycemia (Supplementary Figs. 3D and 3E). Oral tolerance was induced in STZ-treated mice by a single gavage with 10 mg OVA. Interestingly, treatment with STZ disturbed oral tolerance induction, as shown by no difference in anti-OVA IgG1 and total IgE levels compared to nontreated mice (Supplementary Figs. 3F and 3G). Additionally, STZ treatment abrogated the increased frequency of CD4$^+$Foxp3$^+$ cells in the mLN after oral tolerance induction (Supplementary Fig. 3H).

To determine whether the failure of oral tolerance induction in our diet-induced obesity model was attributed to hyperglycemia or obesity itself, we administered metformin, a glycemic modulator, to obese mice. Metformin was administered in the drinking water at a concentration of 1 g/l for 28 days, aiming to reduce fasting glucose levels to those comparable to lean control mice (Fig. 3A and 3B). Despite the treatment, obese mice still exhibited higher body weights than the lean control group (Fig. 3C). Our results revealed that metformin-treated obese mice exhibited a recovery of gut permeability to basal levels (Fig. 3D), indicating that hyperglycemia, rather than obesity itself, may play a key role in the failure of oral tolerance induction observed in our diet-induced obesity model. The treatment restored their ability to develop oral tolerance upon OVA gavage, indicated by reduced levels of anti-OVA IgG1 and total IgE (Fig. 3E and 3F). Mice treated with metformin were not able

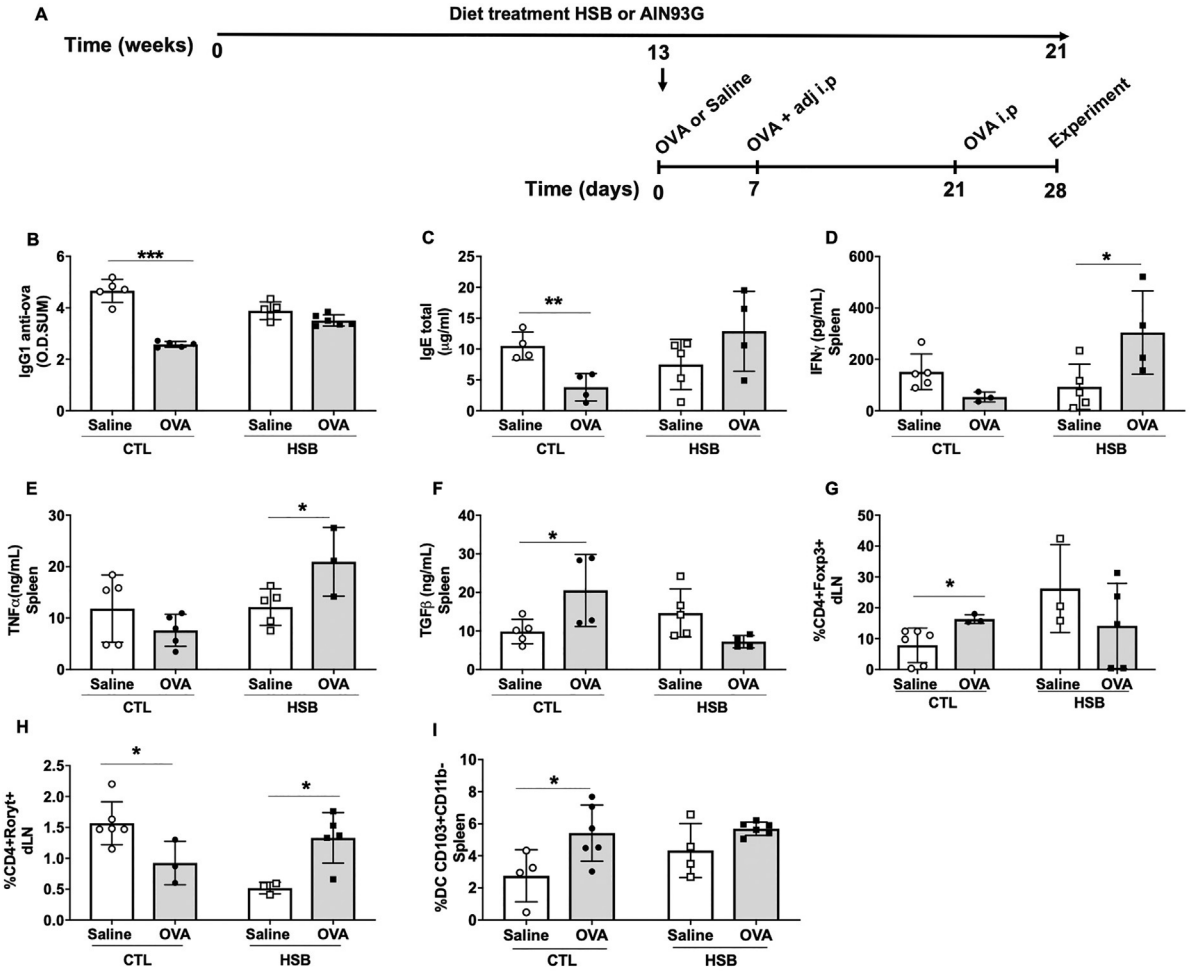

Fig. 2 Diet-induced obesity disturbs oral tolerance induction. (A) Experimental design for oral tolerance induction. Mice received either AIN93G or HBS diet for 13 weeks; then mice received an intragastric injection with 10 mg of OVA or saline, after 7 days, mice received an i.p injection containing 10 µg of OVA in 1 mg/ml of $Al(OH)_3$; a booster with 10 µg OVA in saline was given i.p. 14 days later and 7 days thereafter, mice were bled, and serum was collected for antibody assays. (B) Serum anti-OVA antibodies IgG1 were measured by enzyme-linked immunosorbent assay. The results are expressed as arithmetic mean ± standard deviation from the sum of the OD of the serial dilutions (O.D. SUM). (C) Serum levels of total IgE measured by enzyme-linked immunosorbent assay. (D–F) Cytokines from spleen cell culture supernatant stimulated with OVA during 72 hours (IFN-γ, TNF-α, and TGF-β). (G and H) Frequency of $CD4^+Foxp3^+$ Treg cells and $CD4^+Ror\ \gamma t^+$ in the duodenal lymph nodes (dLN) after oral tolerance induction analyzed by flow cytometry (each point represents two mice). (I) Frequency of DC $CD103^+CD11b^-$ in the spleen after oral tolerance induction analyzed by flow cytometry. Graphics are representative of an individual experiment performed at least three times (N = 4 to 12). (*) indicates $p < 0.05$ analyzed by two-way analysis of variance. White bars represent mice that received only saline by gavage and grey bars represent mice that received OVA by gavage. Circles represent lean control mice, and squares represent obese mice. CD = clusters of differentiation; CTL = lean control mice; DC = dendritic cells; HSB = high-sugar and high-fat die; IFN = interferon; Ig = immunoglobulin; i.p = intraperitoneal; OVA = ovalbumin; TGF = transforming growth factor; TNF = tumor necrosis factor.

to increase the frequency of $CD4^+Foxp3^+$ cells (Fig. 3G). However, an increased frequency of $CD4^+GATA3^+$ cells (Fig. 3H) and a reduced frequency of $CD4^+T\text{-}bet^+$ cells (Fig. 3I) were observed, and the same result was observed in the lean control mice.

We observed a significant alteration in the gut microbiota composition of obese mice following HSB diet feeding (Supplementary Figs. 4A and 4B). To investigate whether microbiota alteration contributes to the failure of oral tolerance induction in obese mice with hyperglycemia, we administered an antibiotic cocktail to both lean control mice and obese mice. Antibiotic treatment restored fasting blood glucose, gut permeability, and oral tolerance induction in both groups (Supplementary Figs. 4C–H). Therefore, these results suggest that hyperglycemia is an important disturbing factor for the breakdown in intestinal homeostasis, affecting oral tolerance induction, rather than excess body weight itself.

Obesity aggravated food allergy in mice

Oral tolerance to food antigen failure may impact the development of food allergies. To determine the influence of obesity on food allergy to OVA and whether glycemic index control could influence the immune response to orally derived antigens, we treated obese mice with metformin (1 g/l) in drinking water for 28 days (Fig. 4A). Metformin treatment improved fasting blood glucose (Supplementary Fig. 5A) and glucose tolerance

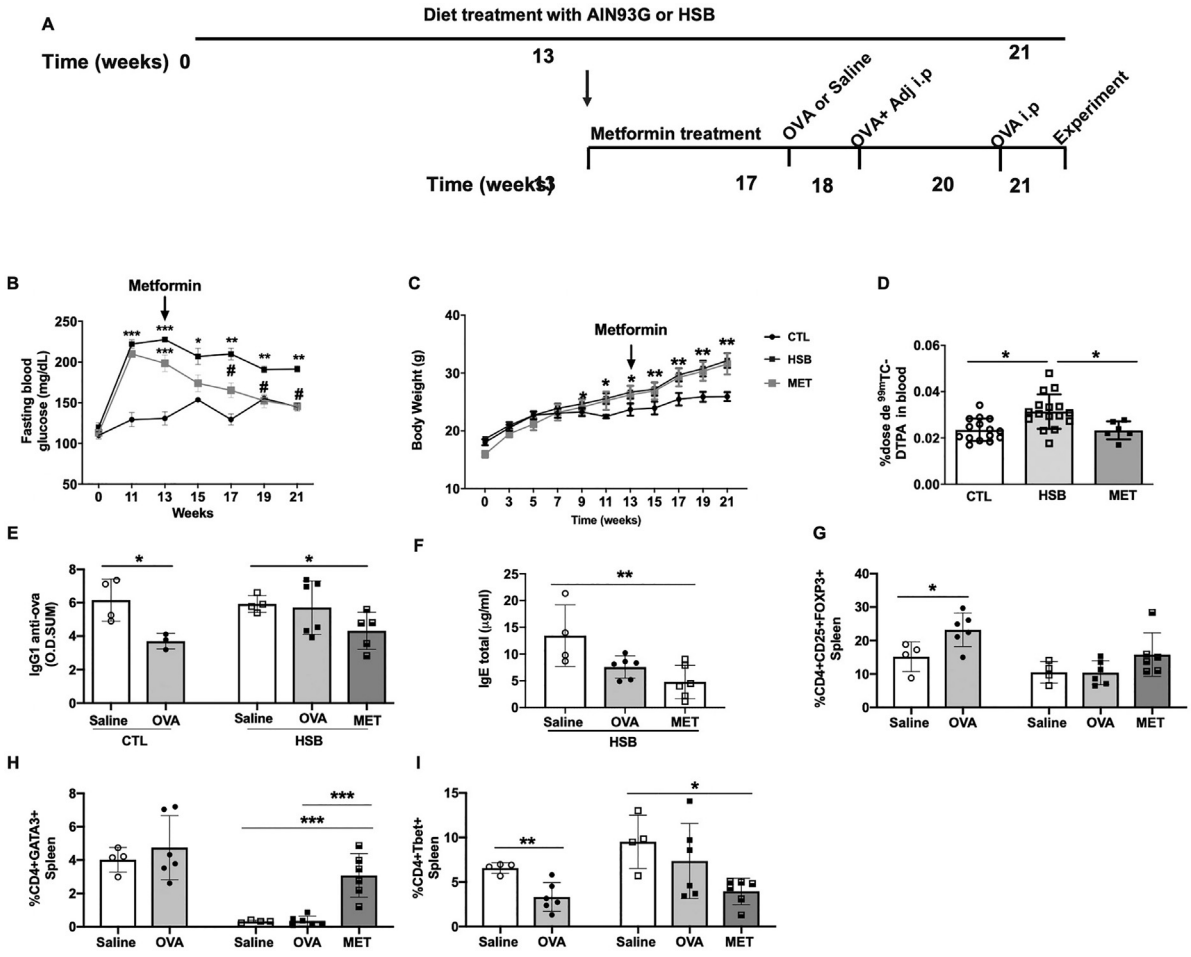

Fig. 3 Hyperglycemia control by Metformin restored oral tolerance induction in obese mice. (A) Experimental design: obesity induced by HSB diet consumption for 13 weeks followed by Metformin treatment (1 g/l dissolved in their drinking water for 28 days) before oral tolerance induction protocol. The control diet AIN93G or HSB were kept during all experiment. (B) Fasting blood glucose concentration. (*) represents the difference between CTL and other groups (* $p < 0.005$). (#) represents the difference between MET and HSB mice (#p < 0,005). (C) Body weight during 21 weeks. (D) Plasma concentration of ^{99}mTc-DTPA to indicate intestinal permeability. (E) Specific anti-OVA IgG1 in serum of mice after oral tolerance induction measured by enzyme-linked immunosorbent assay. (F) Total IgE in the serum of mice after oral tolerance induction measured by enzyme-linked immunosorbent assay. (G–I) Frequency of $CD4^+CD25^+Foxp3^+$ Treg cells, $CD4^+GATA3^+$, and $CD4^+Tbet^+$ in the spleen after oral tolerance induction analyzed by flow cytometry. Graphics are representative of an individual experiment performed at least three times. Each symbol indicates an individual mouse ($n = 3$ to 15). (* or #) indicates $p < 0.05$ analyzed by two-way analysis of variance. Groups: control – CTL, obese – HSB, and obese Metformin-treated – MET. ^{99}mTc-DTPA = 99 m-technetium diethylenetriamine penta-acetic acid; CD = clusters of differentiation; CTL = lean control mice; HSB = high-sugar and high-fat die; Ig = immunoglobulin; i.p = intraperitoneal; OVA = ovalbumin.

in obese mice compared with untreated obese mice (Fig. 4B and 4C). Then, food allergy was induced by i.p. immunization with 10 µg OVA plus 1 mg alum followed by oral challenge with 20% OVA solution in a water bottle for 7 consecutive days (Fig. 4A).

The allergic obese mice drank less OVA solution, which was a typical sign of food allergy in this model (Fig. 4D). Obese mice lost weight during the challenge and presented higher gut permeability than obese mice without allergy and obese mice treated with metformin (Fig. 4E and 4F).

More specifically, we tested whether OVA allergy in obese mice could impair anaphylaxis *in vivo* mediated by anaphylactic antibodies. We determined the magnitude of active cutaneous anaphylaxis measured *in vivo* by Evans Blue extravasation upon intradermal injection of OVA. We found that OVA-allergic obese mice developed intense dye extravasation upon intradermal OVA injection when compared to the lean control or allergic metformin-treated (HSB-MET) mice, which showed very discrete dye extravasation (Fig. 4G, Supplementary Fig. 5B). All these results indicate that glucose control in obese mice prevents OVA-specific active cutaneous anaphylaxis. Regarding anti-OVA IgG1 production, all mice sensitized with OVA and alum adjuvant showed a significant increase in serum concentrations (Fig. 4H). However, obese mice treated with metformin had lower serum IgE total levels than obese animals without metformin treatment (Fig. 4I). No differences were observed in the concentrations of IgM and IgG2a in the plasma of these animals (Supplementary Figs. 5C and 5D).

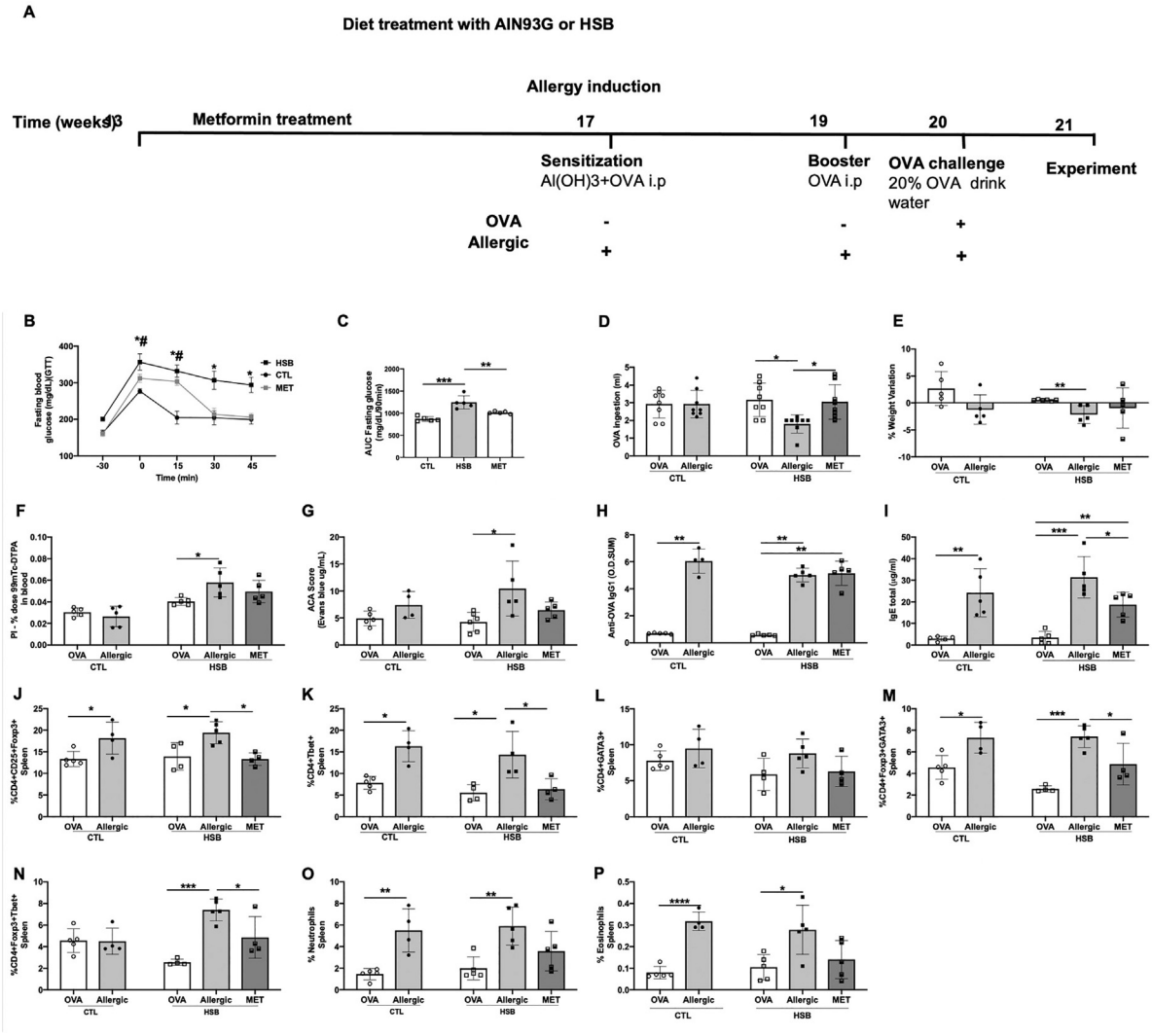

Fig. 4 Obesity aggravates food allergy in mice. (A) Experimental design of obesity induction with HSB diet during 13 weeks, followed by Metformin treatment during 28 days. After Metformin treatment, mice from allergic groups received a s.c. injection with 10 µg OVA and Al $(OH)_3$. The secondary sensitization was induced with s.c. injection of 10 µg of OVA 14 days after the primary sensitization. Seven days after the second injection, mice received an oral challenge with 20% OVA in the water bottle. As control of food allergy protocol, mice did not receive OVA injection before the oral challenge. (B) GTT performed on the 16th week. (C) The area under the curve from GTT. (D) Quantity of OVA solution ingestion. (E) Weight variations of mice up to 21 days after the first sensitization with OVA. (F) Plasma concentration of ^{99}mTc-DTPA to indicate intestinal permeability. (G) Evans Blue dye extraction with formamide after ACA. (H-I) Serum anti-OVA IgG1 and total IgE levels measured by enzyme-linked immunosorbent assay. (J-P) Frequency of $CD4^+CD25^+Foxp3^+$, $CD4^+GATA3^+$, $CD4^+Tbet^+$, $CD4^+Foxp3^+GATA3^+$, $CD4^+Foxp3^+Tbet^+$, Neutrophils, and Eosinophils in the spleen. Each symbol indicates an individual mouse (n = 4 to 6). (*) $p \leq 0.05$ analyzed by two-way analysis of variance. White bars represent mice that received only saline s.c. and oral OVA; grey bars represent mice that received s.c. injection of OVA and Alum and then oral OVA. Dark grey bars mice that received s.c. injection of OVA and Alum and then oral OVA after Metformin treatment. Circles represent lean control mice, and squares represent obese mice. Control lean- CTL, obese – HSB, and obese Metformin-treated – MET. ^{99}mTc-DTPA = 99 m-technetium diethylenetriamine penta-acetic acid; ACA = active cutaneous anaphylaxis; CTL = lean control mice; GTT = glucose oral tolerance test; HSB = high-sugar and high-fat die; Ig = immunoglobulin; i.p = intraperitoneal; OVA = ovalbumin; s.c. = subcutaneous.

In food allergy conditions, obese and lean control mice both had increased frequencies of $CD4^+Foxp3^+$ and $CD4^+$T-bet^+ cells when compared to nonsensitized mice (Fig. 4J and 4K). No difference was observed in $\%CD4^+GATA3^+$ cells (Fig. 4L). Interestingly, obese animals treated with metformin showed similar cell frequencies compared to nonsensitized obese mice. Lean control and obese allergic mice had an increased frequency of $CD4^+Foxp3^+Gata3^+$ cells (Fig. 4M), and the frequency of $CD4^+$-$Foxp3^+$T-bet^+ cells increased only in obese allergic mice (Fig. 4N). However, obese allergic mice treated with metformin (MET) presented a lower frequency of these cell populations than obese allergic mice.

Furthermore, lean control allergic mice and obese allergic mice presented a higher frequency of neutrophils and eosinophils (Fig. 4O and 4P), classical food allergy signals[28]. We also evaluated mast cells by histology, which are critical effectors

of allergic inflammation[29], and we identified an increased number in the jejunum of obese allergic mice (Supplementary Fig. 5E).

Thus, these data confirmed that obesity with hyperglycemia is associated with a more severe food allergy reaction to dietary antigens, possibly related to impairment in oral tolerance induction.

Hyperglycemia associated with obesity was correlated with high IgE levels and gut barrier alterations in humans

Our research focused on the relationship between obesity and food allergies, specifically concerning IgE levels. We observed that oral tolerance induction failed in obese mice, leading to increased severity of food allergies. To investigate whether this finding could be translated to humans, we conducted a study to determine whether IgE levels were correlated with obesity and hyperglycemia. IgE was used as a marker for allergic diseases, as previous studies have shown a correlation between high blood levels of IgE and an allergic predisposition[21,30].

We investigated the relationship between obesity, type 2 diabetes (T2D), gut homeostasis, and allergic diseases by examining circulating IgE levels and gene expression in jejunum biopsies. We studied 60 obese individuals with a body mass index higher than 40 kg/m^2, stratified as patients with obesity and patients with obesity and T2D (see Supplementary Table S1). We found that obese individuals with T2D had higher IgE plasma levels than obese individuals without T2D (Fig. 5A). Additionally, IgE serum levels were positively correlated with glycated hemoglo-

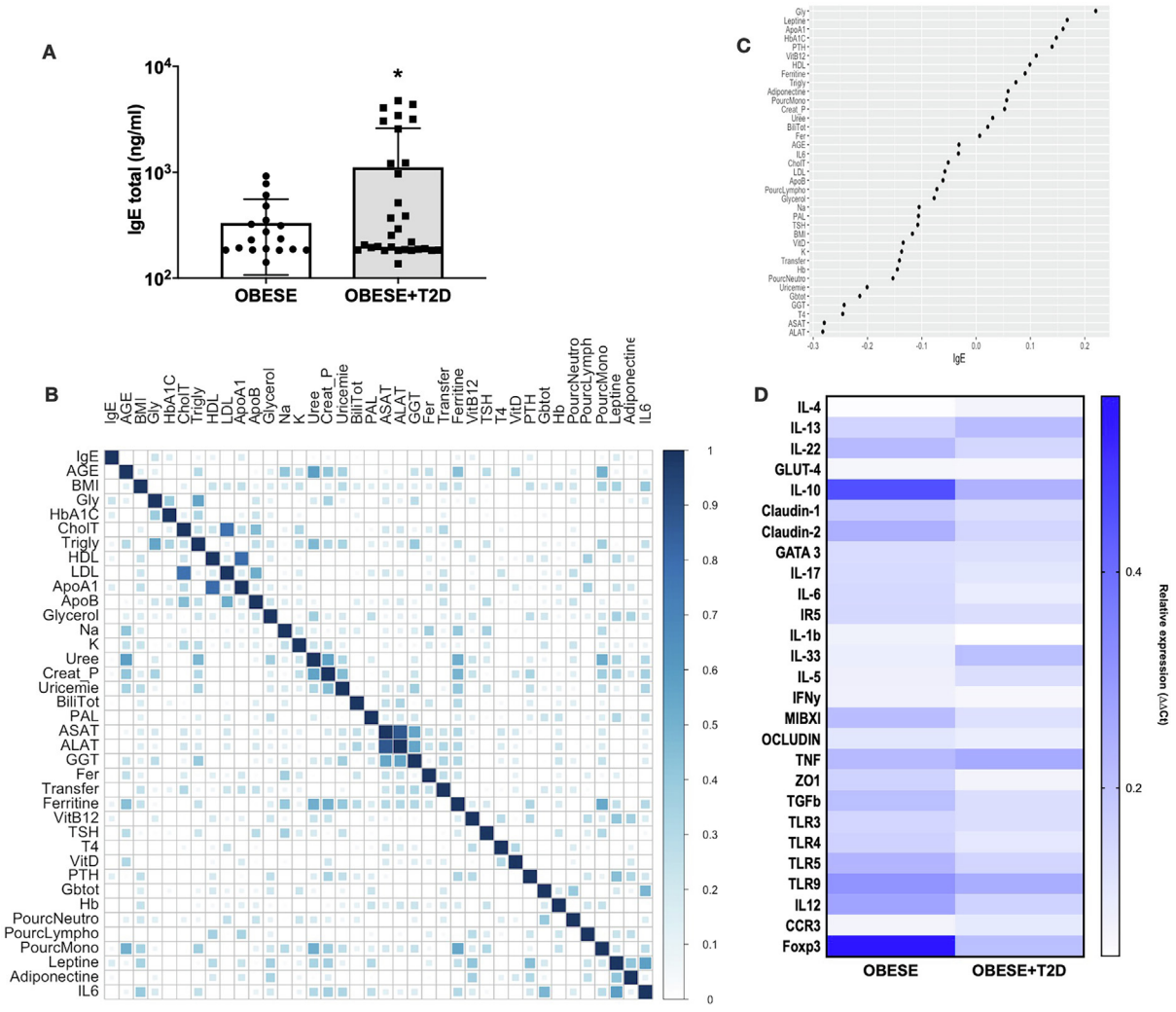

Fig. 5 Hyperglycemia associated with obesity is correlated with high IgE levels and gut alterations in humans. The sample comprised obese patients without T2D (OBESE) and obese patients with T2D (OBESE+T2D). (A) IgE plasma concentration measured by enzyme-linked immunosorbent assay. (B and C) Positive correlation matrix and average correlations IgE levels with biochemistry parameters in the serum of 60 obese patients. Spearman's correlation correlogram. The correlation matrices across all metabolic values, comparing obese and obese with T2D. The strength of the correlation between two variables is represented by the color of the square at the intersection of those variables. Colors range from bright blue (strong positive correlation; i.e. $r^2 = 1.0$). Results were not displayed if $p > 0.05$. (D) Heat map showing relative RNA expression (DDCt) of jejunum biopsies from obese patients without T2D (obese) and obese with T2D (obese+T2D). ALAT = alanine aminotransferase; ASAT = aspartate aminotransferase; BMI = body mass index; GGT = gamma-glutamyl transferase; HbA1C = hemoglobin A1C; HDL = high-density lipoprotein; IFN = interferon; Ig = immunoglobulin; IL = interleukin; LDL = low-density lipoprotein; T2D = type 2 diabetes.

bin and fasting blood glucose in individuals with T2D (Fig. 5B-C), indicating a link between high blood glucose concentration and elevated serum levels of IgE in obese individuals with T2D. We then evaluated gene expression for proteins related to gut homeostasis in jejunum biopsies, comparing obese patients with obese plus T2D patients. We found downregulation of IL-22, IL-10, Foxp3, ZO-1, and claudin-2 and upregulation of IL-33 and IL-5 in obese people with T2D (Fig. 5D). These results are related to increased intestinal permeability and inflammation, suggesting that obesity with T2D can alter gut homeostasis and contribute to the development of allergic diseases.

Together, these findings suggest a possible mechanism linking metabolic diseases to inflammatory conditions, such as allergy, through altered gut homeostasis and higher levels of IgE in obese individuals with T2D.

DISCUSSION

The present study verified that obesity associated with hyperglycemia disturbs intestinal homeostasis due to increased permeability, changes in epithelial cells, and compromised harmony between regulatory and inflammatory cells. These factors compromised oral tolerance and worsened food allergy. Therefore, the treatment of hyperglycemia partially restores intestinal mucosal homeostasis and oral tolerance induction and decreases food allergy symptoms. Similar results were observed in humans, as obese individuals with T2D demonstrated increased IgE serum levels and impairment in intestinal homeostasis.

In general, obesity causes low-grade chronic inflammation that can trigger metabolic dysfunctions and alterations in the immune response, contributing to an increased inflammatory process in the gut mucosa[5]. In the present study, signs of a subclinical inflammatory state in the intestinal mucosa included increased protective mechanisms against bacteria, such as mucus production, intraepithelial lymphocytes (IEL) frequency, and SIgA. Previous reports show that IEL numbers are higher in obese individuals with or without diabetes than in eutrophic people[6]. The increased frequencies of IELs in obesity are correlated with the increased intestinal permeability that favors the dissemination of luminal antigens, microbiota alterations, and inflammation[6,31], and in obesity conditions, there are elevated levels of serum IgA, and the rise in IgA levels is associated with pathogenic bacterial infection or low density lipoprotein (LDL) oxidation[32,33]. In our study, the increase in SIgA levels and IgA-coated bacteria in obese mice was associated with alterations in intestinal microbiota composition with the increased load of potentially pathogenic microbial species in the intestine.

The small intestine presents physiological compartmentalization with different lymphatic drainage and immune cell compositions, which is important in addressing different antigen sources[34,35]. Esterházy et al.[35] showed that mLNs had a specific immunological signature for each intestinal segment. Proximal mLNs (lymph nodes that drain the duodenum and jejunum) preferentially give rise to tolerogenic characteristics due to the presence of tolerogenic DCs ($CD103^+CD11b^-$), favoring the differentiation of naive T cells into $CD4^+Foxp3^+$ iTregs. In contrast, distal lymph nodes favor the differentiation of Th17 Ror γt^+ cells. Interestingly, we observed important alterations in obese mice in the proximal mLNs and in the small intestine lamina propria with a reduced frequency of $CD4^+Foxp3^+$ regulatory T cells (iTregs) and a decreased frequency of $CD103^+CD11b^-$ when compared to lean mice. These cells are involved in oral tolerance induction, which can be a mechanism leading to its failure.

Oral tolerance can be understood as a physiological mechanism driven by immunoregulatory reactivity to diet and microbiota antigens. Oral tolerance is triggered in the intestinal mucosa with systemic repercussions, as it involves controlling specific cellular and humoral responses along the body[9,36]. Here, we identified that oral administration of OVA could not induce oral tolerance in obese mice, as verified by failure to suppress both humoral and cellular responses. The generation of antigen-specific regulatory cells preferentially induces T cells that secrete downmodulatory cytokines such as IL-10 and TGF-β and decreases the production of inflammatory (IFN-γ and TNF-α) cytokines[37]. In our study, we observed that obese mice have an opposite response, where they do not have Th1 cell suppression, with no increased concentration of TGB-β. Increased production of TGF-β has been detected in several studies on oral tolerance, indicating its importance in the development of this phenomenon[37–39]. TGB- β supports Treg cell development and inhibits Th17 cell differentiation in a homeostatic environment[39], which may also be related to increased Th17 frequency and reduced Foxp3 in obese mice after oral OVA treatment. Overall, our findings highlight that obesity affects mucosal homeostasis and, consequently, oral tolerance establishment.

A pivotal question that needs to be addressed is whether the inflammatory events that lead to the breakdown of oral tolerance in the gut mucosa are instigated by metabolic changes, such as hyperglycemia, or by the presence of overweight itself. A previous study described that hyperglycemia impacts gut homeostasis and increases intestinal permeability[25]. Our research team has demonstrated that alterations in gut components can impact oral tolerance induction in nonobese diabetic mice (NOD) used as a model for type 1 diabetes (T1D). Specifically, NOD mice failed to modulate their immune response to OVA. In the current study, in which we used a diet-induced obesity model, our findings suggest that hyperglycemia is the crucial event that triggers disruptions in intestinal homeostasis and ultimately leads to the breakdown of oral tolerance induction. Our hypothesis is supported by the three experimental strategies employed in this study. First, treatment with STZ induced high glucose levels, increased gut permeability, and disturbed oral tolerance induction without increasing adiposity. Second, treatment of obese mice with metformin, a drug that lowers blood glucose levels, improves glycemia, and restores gut permeability and oral tolerance development in obese mice. Third, the depletion of microbiota in obese mice using a cocktail of antibiotics also improved fasting glucose, gut permeability, and the ability to induce oral tolerance. These results suggest that hyperglycemia impacts gut homeostasis by increasing gut permeability and disrupting the immune regulatory response critical to driving oral tolerance development.

One hallmark feature of oral tolerance breakdown is the development of allergic reactions. To investigate whether obesity and hyperglycemia interfere with food allergy development regarding the breakdown in gut homeostasis, we induced food allergy to OVA in obese and obese metformin-treated mice. The results showed that hyperglycemia associated with obesity aggravates the allergic response, as observed by lower ingestion of OVA solution during oral challenge, loss of body weight, anaphylactic reaction, and higher titers of anti-OVA IgG1 and total IgE. Furthermore, obese animals treated with metformin before

food allergy induction responded better to OVA ingestion, with reduced weight loss, decreased dye extravasation, and decreased IgE titers.

Food allergy can manifest as immediate hypersensitivity with specific IgE antibodies bound to mast cells and basophils that compromise immunological balance that drives reactions to ingested antigens. This active process depends on the generation of pro-allergic effector cells[20,40]. In allergic obese mice, we observed an increase in the number of mast cells, frequencies of $CD4^+$T-$bet^{+,}$ and eosinophils. It is important to note that in the C57BL/6 experimental allergy model, we also observed increased activation of the Th1 immune response[64], and metformin treatment also modulated this response. Additionally, we observed an increase in the frequency of $CD4^+Foxp3^+$, $CD4^+$-$Foxp3^+GATA3^+$, and $CD4^+Foxp3^+Tbet^+$ cells in obese allergic mice. These results were previously described where the authors showed an increased frequency of $CD4^+Foxp3^+$ cells in allergic conditions; however, these cells might show functional alterations[41–44]. Recent studies have shown that Foxp3 cells that coexpress other transcription factors characteristic of other phenotypes acquire other functions depending on the environment in which they are present and can negatively influence the disease outcome[43,44]. Nonetheless, treatment of hyperglycemia with metformin reduced all allergic symptoms, suggesting that obesity associated with hyperglycemia is a triggering factor for allergy aggravation.

To explore our hypothesis that obesity in conjunction with hyperglycemia could be linked with intestinal inflammation and allergy occurrence, also in humans, we evaluated biomarkers of gut physiology and measured serum IgE levels in a cohort of obese individuals, categorized as either obese or obese with T2D. Our results demonstrated higher levels of IgE in obese individuals with T2D. This finding confirms our previous hypothesis and suggests a potential association between obesity and increased susceptibility to allergies. Increased serum IgE has been reported in nonallergic diseases in obese humans[45,] and previous studies have shown a positive correlation between obesity, allergic symptoms, and high serum IgE levels in children and adults[24,46–48]. In addition, a study conducted with 8,856 adults in China showed that prediabetic individuals had a positive correlation between high levels of fasting glucose and IgE[48].

We also investigated the expression of genes associated with intestinal homeostasis in jejunal biopsies, and the results showed a negative correlation between hyperglycemia and the expression of genes responsible for maintaining gut homeostasis. Specifically, the mRNA expression of IL-10, IL-22, Foxp3, and claudin was reduced in obese individuals with T2D compared to obese individuals without T2D. IL-22 is associated with intestinal barrier integrity, regulates lipid and glucose metabolism, and contributes to mucosal immunity in diabetic mice[49]**.** Tight junction proteins such as claudin 2 are essential for the control of intestinal permeability[50]. The downregulation of the expression of these genes in obese humans suggests changes in intestinal homeostasis with a possible impact on tolerance development and homeostasis of the intestinal immune response. The genes for the cytokines IL-33 and IL-5 also had higher expression in the jejunum of obese patients with T2D. Both cytokines are associated with allergic diseases such as asthma and food allergy. IL-33 is produced by intestinal epithelial cells upon damage, acting as an alarmin[51]. IL-5 induces the differentiation and growth of eosinophils at sites of inflammation[52].

In humans, the presence of metabolic syndrome is associated with an increased risk for intestinal infections with severe inflammation[53] and a disruption in the regulatory mechanisms responsible for gut homeostasis[54,55]. Hyperglycemia is associated with increased intestinal permeability favoring the contact of dietary and microbiota antigens with immune cells[25,56]. Inflammatory consequences such as oral tolerance breakdown and food allergy development may follow it. Rohmann et al.[57] showed that in the obese population, type I and type IV allergies have a higher prevalence, as indicated by an impaired immune response differentially regulated by an unfavorable lifestyle, microbiota, and metabolic dysfunctions.

One limitation of the human study was the absence of a eutrophic group, as the sample only included obese individuals. However, this does not impact the quality of the study. The results are consistent and show similarities between the findings in mice and humans, suggesting that obesity associated with hyperglycemia may increase susceptibility to allergy by disrupting gut tolerance.

Therefore, maintaining normal glycemia is a critical metabolic component that supports gut health and oral tolerance induction, preventing gut inflammation and allergic diseases. In contrast, hyperglycemia may act as a mechanistic link for various seemingly unrelated inflammatory bowel diseases and allergies associated with obesity[58,59].

CONCLUSION

Our study demonstrated that diet-induced obesity and hyperglycemia can disrupt intestinal homeostasis by increasing gut permeability, impairing regulatory T-cell development and oral tolerance induction, and increasing susceptibility to food allergy. Furthermore, our findings show that obese individuals with type 2 diabetes have increased IgE production, suggesting that hyperglycemia may serve as a link between obesity and allergic diseases.

METHODS

Mice and dietetic treatment

Four-week-old male C57BL/6 mice (average initial weight 20 g) were maintained in the animal care facility of Universidade Federal de Minas Gerais (UFMG) under specific pathogen-free conditions. All mice were housed and had free access to filtered water and food throughout the experiments according to the experimental protocol approved by the Ethics Committee on Animal Care and Use (CEUA-UFMG, Brazil, protocol 335/2017) of UFMG. Groups: CTL – lean control mice that received AIN93G diet; HSB – mice that received HSB diet and became obese; MET – obese mice treated with metformin before oral tolerance induction and immunization; STZ – mice that received streptozotocin (non-obese hyperglycemia model).

Hight sugar and butter diet (HSB)

Mice received during all experimental protocols either the AIN93G[26] diet as a control diet or a hypercaloric diet, HSB, containing high amounts of sugar and butter, according to a previously published study[22].

Measurement of body weight and metabolic parameters

All mice were weighed once a week throughout the experimental period. After 5 and 13 weeks, fasting blood glucose was measured using a capillary glycosometer (Accu—Chek Active, Roche, Basel, Switzerland). For the glucose tolerance test, fasted mice

received 2 g of glucose per kg body weight. Blood was collected from the tail vein, and glucose was measured in mg/dL with a glucometer and strips (Accu—Chek Active, Roche, Basel, Switzerland) 15, 30, 60, and 90 min thereafter.

Gut permeability evaluation

Gut permeability assay was performed after intragastric gavage of 0.1 mL of diethylenetriamine penta-acetic acid labeled with 99 m-technetium (99mTc). After 4 hours, the radioactivity diffusion was measured in the blood using an automated gamma counter (Perkin Elmer. Wallac Wizard 1470–020 Gamma Counter; PerkinElmer Inc., Waltham, MA, USA). The obtained results were compared with the standard dose and calculated as a percentage of the dose per gram of blood using the following equation: %dose/g blood= (cpm of blood/cpm dose of standard) × 100; where cpm represents the counts of radioactivity per minute[60].

Enzyme-linked immunosorbent assay (ELISA)

ELISA determined anti-OVA IgG1 serum antibody according to antibody manufacture protocol, and the anti-OVA-IgG1 (Southern Biotechnology, Birmingham, AL, USA) titer was calculated as described previously[10]. Secreted IgA (sIgA) was measured in the feces. The feces were collected and diluted at 100 mg/ml in phosphate-buffered saline (PBS), then centrifuged for 20 minutes, 4000 RPM, at 4 °C. The sIgA concentration was measured in Nunc Maxi Sorp 96-well ELISA plate coated overnight with purified anti-mouse IgA mAb UNLB (1:10000) (Southern Biotechnology, Birmingham, AL, USA) diluted in sodium carbonate buffer, pH 9.6, at 4 °C. Plates were washed with PBS containing 0.05% Tween 20 and blocked for 1 hour at room temperature with PBS containing 0.25% casein. Plates were incubated for 1 hour at room temperature with samples. Then, HRP anti-IgA mAb (Southern Biotechnology, Birmingham, AL, USA); 0.5 mg/ml) was added, and plates were incubated for 1 hour at 37 °C. The reaction was developed at room temperature with 100 µl/well of 2,2′- azino-bis (3-ethylbenzthiazoline-6-sulfonic acid [ABTS, Sigma-Aldrich, São Paulo, SP, Brazil) and H_2O_2 substrate in sodium citrate buffer. The reaction was interrupted with the addition of 20 µl/ well of SDS1%. Absorbance was measured by an ELISA reader (Bio-Rad Model 450 Microplate Reader, Hercules, CA, USA) at 405 nm. Matched antibody pairs were used for measuring TGF-β, IL-10, IFN-γ, and TNF-α by ELISA (DuoSets, R&D Systems, Minneapolis, MN, USA) using each specific standard according to the manufacturer's protocol.

Analysis of IgA-coated bacteria

Feces from the colon were collected and transferred to a plastic tube, where they were diluted in sterile PBS (100 mg/ml). Homogenates were centrifuged for 20 minutes, 400 g, at 4 °C. Supernatants were collected, filtered through a 70 µm cell strainer, diluted (1:1000) in PBS, and centrifuged at 8000 g to precipitate bacteria. Pellets obtained were incubated with and without FITC-labeled goat F(ab)2 anti-mouse IgA for 20 min. Samples were analyzed by flow cytometry (BD FACSCanTM).

Cell culture preparation

mLN and spleen were removed, and cell suspensions were prepared using a tissue homogenizer and centrifuged. Spleen red cells were lysed, and the suspension was centrifuged to isolate leukocytes. Isolated cells were cultured at 5×10^6 cells/ml in RPMI 1640 medium (Life Technologies, Carlsbad, CA, USA) enriched with 2 nM L-glutamine, 50 mM 2-mercaptoethanol, 100 U/ml penicillin, 1 mM sodium pyruvate, 0.1 mM non-essential amino acids, 25 mM HEPES, and 10% inactivated fetal bovine serum (FBS) (Cold Lab, Campinas, SP, Brazil) and stimulated with OVA (10 µg/ml) for cytokine secretion analyses. Supernatants were collected after 72 hours to measure TNF- α, IFN- γ, and TGF-β cytokines by ELISA.

Flow cytometry analysis

CD4 T lymphocytes, dendritic cells (DCs), ILCs, and IEL extracted from either mLN, *lamina propria*, or spleen were evaluated by flow cytometry. Cells were incubated in polystyrene tubes with anti-CD16/CD32 mAb to block Fc RII/III receptors and stained on ice for 30 minutes and for more than 30 minutes at 4 °C with live/dead reaction. Then, cells were washed and incubated with 20–30 µl of a fluorochrome-labeled antibody mix for 40 minutes at 4 °C to stain for cell surface molecules. For intracellular labeling of Foxp3, GATA3, RORγt, and T-bet transcription factors, a commercial fixation/permeabilization kit (e-Bioscience, San Diego, CA, USA) was used and samples were incubated for another 30 minutes with fluorochrome-labeled antibodies. After washing with PBS- BSA (0.5% BSA), samples were acquired at either FACSCanto II or FACSFortessa (BD Biosciences, San Jose CA, USA) coupled to computers with Diva software for flow cytometry analysis. Populations of interest were delimited by size and granularity (Forward Scatter × Side Scatter), and 50.000 or 100.000 events were acquired for subsequent analysis using FlowJo software.

Fluorescent-dye-conjugated monoclonal antibodies (mAbs) were anti-mouse CD8α, 60-0081-U100, Pe-Cy7 (53-6.7); anti-mouse CD45 103108, FITC (30- F11); anti-mouse CD8b, 37 48-0083-80, Efluor 450 (eBioH35-17.2); anti-mouse TCR β, 109227, PerCP-Cy 5.5 (H57-597); LIVE/DeadTM Fixable Aqua Stain Kit, L34957; anti-mouse CD4, 17-0041-82, APC (GK1.5); anti-CD45, 25-0451-82, PE/Cy 7 (30-F11); anti-Foxp3, 12-5773-82, Pe (FJK-16s); anti-mouse CD3, 555276, PE-cy5 (17A2), anti-T-bet, 561267, alexa Fluor 647 (04-68); CD11c, 117322, pacific blue (N414); anti-mouse Roryt, 562697, PE (Q13-378); anti-mouse GATA3, 560405, Pe Cy 7 (L50-823); anti-Foxp3, 560403, alexa fluor 488 (MF23); Streptavidin, 562284, PE-CF594; anti-Ly6G, 560403, BV 605 (1A8-ly6g); anti-Ly6C, 560525, Percp5.5(AL-21); anti-F4/80, 123114,PeCy7 (BM8); anti-TCR, 109222, PeCy7 (H57-597; anti-CD3, 100218, Percp5.5 (17A2); anti-CD19, 553784, BIOTIN (123); anti-CD11c, 561241, APC-cy7 (HL3); anti-CD11b, 553310; anti-CD11b, 553312 (M1/70); CD103, 557494, FITC (M290); anti-TCR, 109222, PeCy7 (H57-597); anti-CD3, 100218, Percp5.5 (17A2); anti-CD19, 553784, BIOTIN (123); anti-CD11c, 561241, APC-cy7 (HL3); anti-CD11b, 553312 (M1/70) APC; CD103, 557494, FITC (M290); anti-CD45, 25-0451-82, PE/Cy7; anti-mouse CD127, 48-1271-80, eFluor 450; anti-mouse T-bet 644813, APC; CD19, 15-0193-82, PerCP-Cy5.5 and rat anti-mouse CD11b, 550993, PerCP-Cy 5.5.

Oral tolerance induction

Crystallized egg OVA grade V (Sigma-Aldrich, St. Louis, MO, USA) was used as antigen. Oral tolerance was induced by single intragastric administration (gavage) with 10 mg OVA in 0.2 ml saline using a round-tip 18-gauge stainless animal feeding needle (Thomas Scientific, Swedesboro, NJ, USA). Control mice received only saline by gavage. Seven days after oral treatment, all mice were injected i.p. with 10 µg OVA in 1 mg of $Al(OH)_3$ (Aluminum Hydroxide, Hortolandia, SP, Brazil) as an adjuvant. A booster with

10 µg OVA in saline was given i.p. 14 days after the first immunization, and 7 days later, mice were euthanized for analysis.

Food allergy induction

Food allergy to OVA was induced using a protocol previously described by SALDANHA 44. Mice were immunized intraperitoneally with 10 µg OVA in 1 mg $Al(OH)_3$ (Aluminum Hydroxide, Hortolandia, SP, Brazil) in 0.2 ml saline. A booster with 10 µg OVA in 0.2 ml saline was given after 14 days, and 7 days after the immunization, water bottles used in the cages were replaced by bottles containing a 20% OVA solution for 7 consecutive days. Mice weight and OVA intake were measured daily.

Active cutaneous anaphylaxis assay

Mice were sensitized to OVA and challenged with egg white solution in their drinking bottle for 7 days. The animals received an intradermal injection (i.d) on the back-containing OVA (20 µg) or PBS, followed by an intravenous at the tail of Evans Blue dye (1 mg/ml). After 30 minutes, the mice were euthanized, and the skin was removed for visualization[61].

Quantitative reverse transcription-polymerase chain reaction

RNAs from human jejunal biopsies were prepared using RNeasy Tissue kit (Qiagen, Germantown MD, USA), and cDNAs were synthesized using SuperScript II and random hexamers (Promega, Madison, WI, USA). Quantitative polymerase chain reaction with SybrGreen was performed, and relative quantification of each transcript compared to the medium of 18s and GAPDH (glyceraldehyde 3-phosphate dehydrogenase)was determined using the 2^(-Delta Delta Ct) method78. All primer sequences are available in the supplementary Table.

Isolation of fecal content and microbiota DNA from feces

Fecal DNA was extracted from fresh mouse fecal samples using the QIAamp DNA Stool Mini Kit (QIAGEN, Hilden, Germany). DNA sequencing of microbiota was performed in the DNA purified from feces was amplified at the V3–V4 hypervariable region of RNA ribosomal 16S and sequenced using the Illumina-MiSeq platform (Illumina, San Diego, CA), which provided single-end reads with 150 nt in length. Downstream analysis was performed by running the QIIME (Quantitative Insights into Microbial Ecology) pipeline. Briefly, sequence reads that presented Phred quality score smaller than 20 were removed. We normalize each library relative to the smaller sample, choosing randomly until it matches its total number of readings. Afterward, representative sequences were grouped by Uclust into Operational Taxonomic Units by 97% similarity and taxonomy assigned with Pynast against the Green genes database. The microbiome profile of mice samples was assessed through relative expression of Filo and Family.

Human subjects

Jejunum biopsy samples were obtained from 60 subjects with severe obesity who met the recruitment criteria for bariatric surgery 79. As part of usual patient care, the BARICAN cohort is recruited and followed up at the Pitié-Salpêtrière Hospital Nutrition Department (Paris, France). In agreement with ethical regulation, patients provided informed consent and are part of several studies registered on https://clinicaltrials.gov (P050318 Les Comités de Protection des Personnes (CPP) approval: 24 November 2006, NCT01655017, NCT01454232)78. This cohort also got approval by CNIL (Commission Nationale de l'Informatique et des Libertés; No. 1222666) and the French Ministry of Research. All patients met standard bariatric surgery indications and are monitored according to national and international guidelines. Patients were not involved in this work's design, conduct, reporting, or dissemination plans. Before bariatric surgery, height and weight were measured by standard procedures. Blood samples were collected after 12 hours of overnight fasting 79. The clinical data of these individuals are described in S1. Insulin resistance was estimated by calculating HOMA-IR as (glucose [nmol/l]*insulin [mU/ml]/22.5) using fasting values80. T2D was diagnosed in accordance with American Diabetes Association (ADA)definition[62]. Serum samples were collected at the fasting state for IgE evaluation. After clinical and biological evaluation, patients were all operated on in the visceral surgery department of Pitié-Salpêtrière hospital in Paris.

Detection of serum IgE levels

Human serum IgE levels were measured by ELISA according to the manufacturer's protocol (IgE ELISA kits; cat. no. BMS2097).

Statistical analysis

Statistical analysis was performed using GraphPad Prism software version 6.0 (La Jolla, CA). Differences between control lean and HSB obese at matching ages were analyzed by Student's t test when there were two groups or analysis of variance and Tukey's test for the experiments with more than two groups. A p value of less than 0.05 was considered significant. Human sample analyses were performed with the Kruskal-Wallis test. A Pearson correlation was performed to identify correlation between mice gut permeability and fasting blood glucose levels. Spearman's correlation graphs were used to assess the association between human numerical variables to try to estimate the strength of this relationship. In correlated data, a change in the magnitude of variables associated with a change in the magnitude of another variable, either in the same direction (positive correlation) Correlation coefficients range from 0 to +1, where 0 indicates no association, while the correlation becomes more positive as it approaches +1. To ensure a definitive conclusion regarding the strength of the relationship between the variables, we did not calculate a confidence interval. Instead, we evaluated only one correlation based on the intensity of the blue color in the present study.

AUTHOR CONTRIBUTIONS

LT and TUM designed the study and wrote the manuscript. LT, MCGM, VMD, SOA, LM, MAO, HC, EG, and NPR performed the experiments in mice. GM, FM, KC, and LT performed the assays in human samples. FCM and LT performed the microbiota analysis. FM, GM, and LT helped with polymerase chain reaction analysis. TUM, AMCF, MR, and GM supervised the project. All authors provided critical comments on the study.

DECLARATIONS OF COMPETING INTEREST

The authors have no competing interests to declare.

FUNDING

This work was supported by research grants from Fundação de Apoio à Pesquisa do Estado de Minas Gerais - FAPEMIG ((APQ 00704-14, RED 00140-16) and Pro-Reitoria de Pesquisa (PRPq) UFMG. LT, VMD, MAO, and LMT are recipients of scholarships, and TUM, MR, and AMCF are fellowships from Conselho Nacional

de Desenvolvimento Científico e Tecnológico (CNPq). NPR and HC are recipients of scholarships from Coordenação de Aperfeiçoamento de Pessoal de Nível Superior (CAPES). We acknowledge the Fondation pour la Recherche Medicale, the French National Agency of Research (Captor program), the European Foundation for the Study of Diabetes, the research program CAPES (Coordenação de Aperfeiçooamento de Pessoal de Nível Superior)/COFECUB (Comité Français d'Évaluation de la Coopération Universitaire et Scientifique avec le Brésil), as well as Novo Nordisk foundation (Jacobaus prize to KC).

COMPLIANCE WITH ETHICAL STANDARDS

Mice: Procedures and manipulation of animals followed the guidelines of the ethics committees in research of Universidade Federal de Minas Gerais in agreement with guidelines of the ethics committees in research from Brazilian Federal Law #11794, October 8th, 2008: http://www.planalto.gov.br/ccivil_03/_ato2007-2010/2008/lei/l11794.htm. All mice experiments were approved by the Committee on Animal Experiments (CETEA) under protocol 335/2017.

Humans: https://clinicaltrials.gov (P050318 Les Comités de Protection des Personnes (CPP) approval: 24 November 2006, NCT01655017, NCT01454232)[63]. This cohort also got approval by CNIL (Commission Nationale de l'Informatique et des Libertés; No. 1222666) and the French Ministry of Research.

ACKNOWLEDGMENT

We thank Dr. Judith Aron-Wisnewsky, and Prof Christine Poitou (nutrition department, Pitié-Salpêtrière hospital, Paris) for patients' recruitment, and Dr Florence Marchelli for patients' data management. Leda Quercia Vieira, Leonardo Vaz, and Ana Elisa Nolasco for the use of her laboratory's equipment. Ilda Marçal and Hermes Ribeiro for mice facility care. Adaliene de Matos Versiane Ferreira to coordinate the Capes-COFECUB program.

APPENDIX A. SUPPLEMENTARY DATA

Supplementary data to this article can be found online at https://doi.org/10.1016/j.mucimm.2023.05.008.

REFERENCES

1. Sun, K., Kusminski, C. M. & Scherer, P. E. P. Adipose tissue remodeling and obesity. *J Clin Invest* **121**, 2094–2101 (2011).
2. Cinti, S. et al. Adipocyte death defines macrophage localization and function in adipose tissue of obese mice and humans. *J Lipid Res* **46**, 2347–2355 (2005).
3. Kusminski, C. M., Bickel, P. E. & Scherer, P. E. Targeting adipose tissue in the treatment of obesity-associated diabetes. *Nat Rev Drug Discov* **15**, 639–660 (2016).
4. Statovci, D., Aguilera, M., MacSharry, J. & Melgar, S. The impact of western diet and nutrients on the microbiota and immune response at mucosal interfaces. *Front Immunol* **8**, 838 (2017).
5. Luck, H. et al. Regulation of obesity-related insulin resistance with gut anti-inflammatory agents. *Cell Metab* **21**, 527–542 (2015).
6. Monteiro-Sepulveda, M. et al. Jejunal T cell inflammation in human obesity correlates with decreased enterocyte insulin signaling. *Cell Metab* **22**, 113–124 (2015).
7. Moog, F. The lining of the small intestine. *Sci Am* **245**, 154–179 (1981).
8. Faria, A. M. C. & Weiner, H. L. Oral tolerance and TGF-beta-producing cells. *Inflamm Allergy Drug Targets* **5**, 179–190 (2006).
9. Pinheiro-Rosa, N. et al. Oral tolerance as antigen-specific immunotherapy. *Immunother Adv* **1**, ltab017 (2021).
10. Oliveira, R. P., Santiago, A. F., Ficker, S. M., Gomes-Santos, A. C. & Faria, A. M. C. Antigen administration by continuous feeding enhances oral tolerance and leads to long-lasting effects. *J Immunol Methods* **421**, 36–43 (2015).
11. Castro-Junior, A. B. et al. Oral tolerance correlates with high levels of lymphocyte activity. *Cell Immunol* **280**, 171–181 (2012).
12. Matteoli, G. et al. Gut CD103+ dendritic cells express indoleamine 2,3-dioxygenase which influences T regulatory/T effector cell balance and oral tolerance induction. *Gut* **59**, 595–604 (2010).
13. Esterházy, D. et al. Classical dendritic cells are required for dietary antigen–mediated induction of peripheral T(reg) cells and tolerance. *Nat Immunol* **17**, 545–555 (2016).
14. Zhang, X., Izikson, L., Liu, L. & Weiner, H. L. Activation of CD25(+)CD4(+) regulatory T cells by oral antigen administration. *J Immunol* **167**, 4245–4253 (2001).
15. Mucida, D. et al. Oral tolerance in the absence of naturally occurring Tregs. *J Clin Invest* **115**, 1923–1933 (2005).
16. Weiner, H. L. Oral tolerance: immune mechanisms and the generation of Th3-type TGF-beta-secreting regulatory cells. *Microbes Infect* **3**, 947–954 (2001).
17. Stephen-Victor, E. & Chatila, T. A. Regulation of oral immune tolerance by the microbiome in food allergy. *Curr Opin Immunol* **60**, 141–147 (2019).
18. Lopes, J. P. & Sicherer, S. Food allergy: epidemiology, pathogenesis, diagnosis, prevention, and treatment. *Curr Opin Immunol* **66**, 57–64 (2020).
19. Hussain, M. et al. High dietary fat intake induces a microbiota signature that promotes food allergy. *J Allergy Clin Immunol* **144**, 157–170.e8 (2019).
20. Renz, H. et al.. *Food allergy Nat Rev Dis Primers* **4**, 17098 (2018).
21. Gould, H. J. & Sutton, B. J. IgE in allergy and asthma today. *Nat Rev Immunol* **8**, 205–217 (2008).
22. Maioli, T. U. et al. High sugar and butter (HSB) diet induces obesity and metabolic syndrome with decrease in regulatory T cells in adipose tissue of mice. *Inflamm Res* **65**, 169–178 (2016).
23. Guerville, M. et al. Western-diet consumption induces alteration of barrier function mechanisms in the ileum that correlates with metabolic endotoxemia in rats. *Am J Physiol Endocrinol Metab* **313**, E107–E120 (2017).
24. Visness, C. M. et al. Association of obesity with IgE levels and allergy symptoms in children and adolescents: results from the National Health and Nutrition Examination survey 2005–2006. *J Allergy Clin Immunol* **123**, 1163–1169.e4 (2009).
25. Thaiss, C. A. et al. Hyperglycemia drives intestinal barrier dysfunction and risk for enteric infection. *Science* **359**, 1376–1383 (2018).
26. Reeves, P. G., Nielsen, F. H. & Fahey, G. C. AIN-93 purified diets for laboratory rodents: final report of the American Institute of Nutrition ad hoc writing committee on the reformulation of the AIN-76A rodent diet. *J Nutr* **123**, 1939–1951 (1993).
27. Miranda, M. C. G. et al. Frontline Science: Abnormalities in the gut mucosa of non-obese diabetic mice precede the onset of type 1 diabetes. *J Leukoc Biol* **106**, 513–529 (2019).
28. Shreffler, W. G., Wanich, N., Moloney, M., Nowak-Wegrzyn, A. & Sampson, H. A. Association of allergen-specific regulatory T cells with the onset of clinical tolerance to milk protein. *J Allergy Clin Immunol* **123**, 43–52.e7 (2009).
29. Burchett, J. R. et al. Targeting mast cells in allergic disease: current therapies and drug repurposing. *Cells* **11**, 3031 (2022).
30. Sampson, H. A. et al. Mechanisms of food allergy. *J Allergy Clin Immunol* **141**, 11–19 (2018).
31. Park, C. et al. Obesity modulates intestinal intraepithelial T cell persistence, CD103 and CCR9 expression, and outcome in dextran sulfate sodium-induced colitis. *J Immunol* **203**, 3427–3435 (2019).
32. Vehkala, L. et al. Plasma IgA antibody levels to malondialdehyde acetaldehyde-adducts are associated with inflammatory mediators, obesity and type 2 diabetes. *Ann Med* **45**, 501–510 (2013).
33. Cong, Y., Feng, T., Fujihashi, K., Schoeb, T. R. & Elson, C. O. A dominant, coordinated T regulatory cell-IgA response to the intestinal microbiota. *Proc Natl Acad Sci U S A* **106**, 19256–19261 (2009).
34. Coombes, J. L. et al. A functionally specialized population of mucosal CD103+ DCs induces Foxp3+ regulatory T cells via a TGF-beta and retinoic acid-dependent mechanism. *J Exp Med* **204**, 1757–1764 (2007).
35. Esterházy, D. et al. Compartmentalized gut lymph node drainage dictates adaptive immune responses. *Nature* **569**, 126–130 (2019).
36. da Cunha, A. P. & Weiner, H. L. Induction of immunological tolerance by oral anti-CD3. *Clin Dev Immunol* **2012**:425021.
37. Faria, A. M. C. et al. Oral tolerance induced by continuous feeding: enhanced up-regulation of transforming growth factor-beta/interleukin-10 and suppression of experimental autoimmune encephalomyelitis. *J Autoimmun* **20**, 135–145 (2003).
38. Faria, A. M. C. & Weiner, H. L. Oral tolerance: therapeutic implications for autoimmune diseases. *Clin Dev Immunol* **13**, 143–157 (2006).
39. Mucida, D. et al. Reciprocal TH17 and regulatory T cell differentiation mediated by retinoic acid. *Science* **317**, 256–260 (2007).
40. Saldanha, J. C. S. et al. A model of chronic IgE-mediated food allergy in ovalbumin-sensitized mice. *Braz J Med Biol Res* **37**, 809–816 (2004).
41. Jartti, T. et al. Association between CD4(+)CD25(high) T cells and atopy in children. *J Allergy Clin Immunol* **120**, 177–183 (2007).

42. Hartl, D. et al. Quantitative and functional impairment of pulmonary CD4+CD25hi regulatory T cells in pediatric asthma. *J Allergy Clin Immunol* **119**, 1258–1266 (2007).
43. Noval Rivas, M., Burton, O. T., Oettgen, H. C. & Chatila, T. IL-4 production by group 2 innate lymphoid cells promotes food allergy by blocking regulatory T-cell function. *J Allergy Clin Immunol* **138**, 801–811.e9 (2016).
44. Koch, M. A. et al. T-bet(+) Treg cells undergo abortive Th1 cell differentiation due to impaired expression of IL-12 receptor β2. *Immunity* **37**, 501–510 (2012).
45. Galli, S. J. & Tsai, M. IgE and mast cells in allergic disease. *Nat Med* **18**, 693–704 (2012).
46. Huang, S. L., Shiao, G. M. & Chou, P. Association between body mass index and allergy in teenage girls in Taiwan. *Clin Exp Allergy* **29**, 323–329 (1999).
47. Julia, V., Macia, L. & Dombrowicz, D. The impact of diet on asthma and allergic diseases. *Nat Rev Immunol* **15**, 308–322 (2015).
48. Wang, H. et al. The association between immunoglobulin concentrations and prediabetes prevalence in a large Chinese cohort. *Metabolism* **73**, 77–84 (2017).
49. Wang, X. et al. Interleukin-22 alleviates metabolic disorders and restores mucosal immunity in diabetes. *Nature* **514**, 237–241 (2014).
50. Ahmad, R., Rah, B., Bastola, D., Dhawan, P. & Singh, A. B. Obesity-induces organ and tissue specific tight junction restructuring and barrier deregulation by claudin switching. *Sci Rep* **7**, 5125 (2017).
51. Liew, F. Y., Girard, J. P. & Turnquist, H. R. Interleukin–33 in health and disease. *Nat Rev Immunol* **16**, 676–689 (2016).
52. Kandikattu, H. K., Upparahalli Venkateshaiah, S. & Mishra, A. Synergy of interleukin (IL)-5 and IL-18 in eosinophil mediated pathogenesis of allergic diseases. *Cytokine Growth Factor Rev* **47**, 83–98 (2019).
53. Muller, L. M. A. J. et al. Increased risk of common infections in patients with type 1 and type 2 diabetes mellitus. *Clin Infect Dis* **41**, 281–288 (2005).
54. Rainone, V. et al. Upregulation of inflammasome activity and increased gut permeability are associated with obesity in children and adolescents. *Int J Obes (Lond)* **40**, 1026–1033 (2016).
55. Mörkl, S. et al. Gut microbiota, dietary intakes and intestinal permeability reflected by serum zonulin in women. *Eur J Nutr* **57**, 2985–2997 (2018).
56. Schachter, L. M., Peat, J. K. & Salome, C. M. Asthma and atopy in overweight children. *Thorax* **58**, 1031–1035 (2003).
57. Rohmann, N. et al. Differential effects of obesity, hyperlipidaemia, dietary intake and physical inactivity on type I versus type IV allergies. *Nutrients* **14**, 2351 (2022).
58. Belkaid, Y. & Hand, T. W. Role of the microbiota in Immunity and inflammation Yasmine. *Cell* **157**, 121–141 (2015).
59. Beaurepaire, C., Smyth, D. & McKay, D. M. Interferon-γ regulation of intestinal epithelial permeability. *J Interferon Cytokine Res* **29**, 133–144 (2009).
60. Maioli, T. U. et al. Pretreatment with Saccharomyces boulardii does not prevent the experimental mucositis in Swiss mice. *J Negat Results Biomed* **13**, 6 (2014).
61. Nunes, F. P. B. et al. TLR9 agonist adsorbed to alum adjuvant prevents asthma-like responses induced by Blomia tropicalis mite extract. *J Leukoc Biol* **106**, 653–664 (2019).
62. American Diabetes Association (2) Classification and diagnosis of diabetes. *Diabetes Care* **38**, S8–S (2015).
63. Marcelin, G. et al. A PDGFRα-mediated switch toward CD9high adipocyte progenitors controls obesity-induced adipose tissue fibrosis. *Cell Metab* **25**, 673–685 (2017).
64. Lemos, Luísa, et al. "Neuroimmune Circuits Involved in β-Lactoglobulin-Induced Food Allergy." Brain, Behavior, & Immunity - Health, vol. 23, Aug. 2022, https://doi.org/10.1016/J.BBIH.2022.100471.